DEM Simulations of Toner Behavior in the Development Nip of the Océ Direct Imaging Print Process

I.E.M. Severens
Océ Technologies B.V.
Venlo, The Netherlands

Abstract

This paper describes the modeling of the toner behavior in the development nip of the Océ Direct Imaging print process. The discrete element method is used as the simulation tool for a quantitative description of the system. The interaction rules and the associated parameters are determined for the toner particles and the surfaces of the development rollers. The model is validated with print quality results. It is shown that it is possible to achieve quantitative agreement between DEM simulations and experimental print quality results.

Introduction

The Océ Color Technology is called Direct Imaging (DI) and consists of seven separate color units. In each of these DI-units a bitmap image is transferred directly into a visible toner image on a DI-drum. The heart of the image development process is formed by the Direct Imaging unit which is schematically shown in Figure 1. The toner that is used in this development process is mono-component, magnetizable and electrically conductive. Toner on the supply roller behaves as in a conventional monocomponent magnetic brush development system. As a result of a bias voltage between the supply roller and the DI-drum, toner is attracted to and developed on the DI-drum. The toner on the DI-drum then moves along with the DI-drum until it reaches the fixed magnet that is placed inside the imaging roller. The fixed magnet attracts the magnetized toner particles towards the imaging roller. The DI-drum contains an array of conductive ring shaped tracks beneath a dielectric layer. If an image is to be developed, voltages are applied to the ring electrodes and the toner is drawn towards the DI-drum. The resolution in tangential direction, the direction along the ring electrodes, is determined by the duration of the applied imaging potential. In the axial direction, across the ring electrodes, it is the spacing of the ring electrodes that defines the resolution.

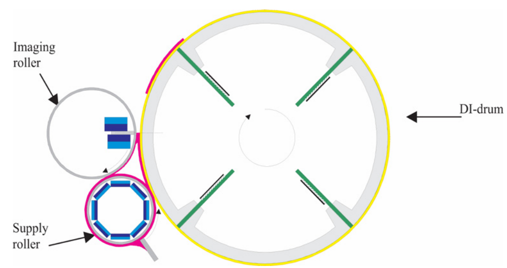

Figure 1. Schematic drawing of a DI-unit.

For each of the seven colors there is a separate DI-unit. The colors of these DI-units are laid down side by side on a rubber coated intermediate cylinder. In the so-called first transfer nip the toner image is transferred from the DI-drum to the intermediate by means of adhesive forces. In the second transfer nip the toner image is transferred and simultaneously fixed and fused onto the receiving medium.

The print quality of the DI technology is primarily determined by the toner flow in the region between the DI-drum and the imaging roller, see Figure 2. The collection of toner between the DI-drum and the imaging roller is called the DI toner assembly. An approach to get insight in the toner flow in the DI-unit is theoretical modeling and numerical simulation. The simulation of toner deposition conducted here is based on the discrete element method, first proposed by Cundall[3] in 1971. In the discrete element method (DEM) all toner particles, as well as the development rollers, are considered discrete elements. Each element interacts with its neighboring elements and its surroundings. These interactions are modeled on a microscopic scale: the motion of each particle is tracked numerically. Every time step the forces that act on a particle are summed and from this the speed and the displacement of the particle is calculated by integration of Newton's second law of motion. The macroscopic behavior of the toner flow and print output is then simulated using DEM. The discrete element method is used extensively in the success of the DEM method lies in correctly establishing the interaction rules and the associated parameters.

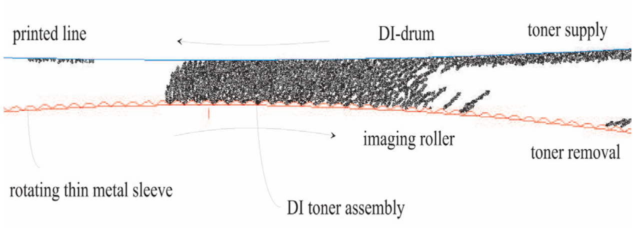

Figure 2. The DI toner assembly.

The model that is developed here is a two-dimensional description of the DI toner assembly. A cross-section of the DI-unit in the direction of the ring electrodes of the DI-drum is described. Our aim is the development of a simulation tool that gives a quantitatively correct description of a toner-like granular medium under the influence of electric and magnetic forces. This tool can support new DI designs.

Force Models

Geometry

In DEM simulations all discrete elements have to be provided with a geometry to indicate the shape of the real object. DEM simulations require the evaluation of inter-element relationships such as contact, distance and relative motion. These operations become increasingly more complicated for complex geometries. In Figure 3, a scanning electron microscopy (SEM) recording of a collection of black toner particles is depicted. A toner particle is described by n clustered spheres, as can be seen in Figure 4. More realistic toner geometries can thus be achieved by increasing the number of clustered spheres that form one toner particle.

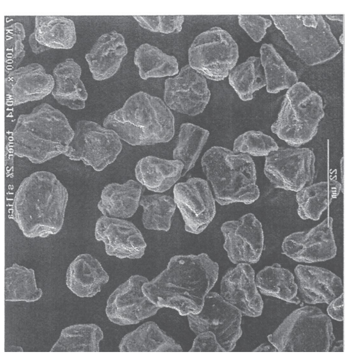

Figure 3. SEM recording of black toner particles.

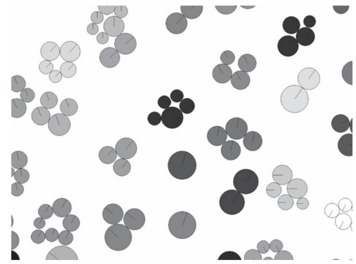

Figure 4. Clustered spheres form one toner particle.

Collisions

DEM simulations involve modeling each collision between particles and between particles and the boundary objects. During a collision with a certain contact time, particles deform, energy is dissipated in the form of heat, and the particles restore to their original shape. A collision is modeled by penetration of the objects during collision. The penetration is described as a certain overlap distance ξ between two objects and models the temporary deformation of the objects during collision. There is a range of contact force models available which approximate the collision dynamics to various extents:

$$F_n = k\xi^{\alpha} - \gamma \frac{d}{dt}\left(\xi^{\beta}\right),$$

where F_n is the normal force between the colliding particles during the collision. The linear spring-dashpot model ($\alpha = \beta = 1$) is a good compromise between physical accuracy and numerical efficiency. The normal dissipation in a collision is characterized by the coefficient of normal restitution which is defined as the ratio between the normal component of the relative velocity before $v_n^{(i)}$ and after $v_n^{(f)}$ the collision,

$$e_n = \left| v_n^{(f)} / v_n^{(i)} \right|./$$

The normal coefficient of restitution of toner is determined by recording a collision between a spherical toner particle (R ≈ 1 mm) with a counter-material (toner, imaging roller, or DI-drum). The contact time is estimated from the collision theory of Hertz.[5]

Collisions between particles are in general not head-on, and the particles have angular velocity. Therefore shear also has to be taken into account. The shear contact force component F_s is generally modeled with a Coulomb friction model:

$$\begin{aligned} F_s &= -\mu_d F_n \operatorname{sign}(v_s) \quad & v_s \neq 0, \\ \left|F_s\right| &<= -\mu_s F_n \quad & v_s = 0 \end{aligned}$$

where μ_s is the coefficient of static friction, F_n the normal force at the contact ($F_n > 0$ always), v_s the relative tangential velocity of the two particles, and μ_d the coefficient of dynamic friction ($\mu_d < \mu_s$). Since Coulomb friction is a discontinuous force model, adjustments have to be made to the model to avoid numerical instability of the force law in a simulation. A simple implementation of the shear contact force is found in Ref. [4]:

$$F_s = -k_s \eta,$$

where k_s is the spring constant of the spring which from time t_0 on, at which the contact was first established, has been stretched over a distance η given by

$$\eta = \int_{t_0}^{t} v_s(\tau) d\tau.$$

The tangential spring force is limited by the maximal static Coulomb friction $\mu_s F_n$; this is the limiting friction that can be withstood by the contact before sliding of one particle over the other commences. In case of sliding, the shear contact force is given by kinetic Coulomb friction $\mu_d F_n$. At that point the spring attaches again at full stretch $\eta = \mu_s F_n / k_s$. The friction coefficient of toner is determined by moving a toner resin sample over a substrate (toner, imaging roller, or DI-drum), and measuring the force that is required to do this. The experimental setups that are used are schematically shown in Figure 5. The motion of both measuring devices consists of two parts. In the first part, where the device moves with a low speed, a so-called stick-slip motion can be observed. The force F_t that is measured is the static friction force.

In the second part, the sample moves with a higher speed over the substrate. Then F_t represents the dynamic friction force. The friction coefficient μ is determined from the force F_t and the gravitational force F_z. For the setup shown in Figure 5a the relation

$$F_t = \mu F_z,$$

holds, and for the setup shown in Figure 5b

$$\frac{F_t}{F_z} = e^{\mu \frac{\pi}{2}}.$$

A often-used choice[7] for the spring constant k_s is $k_s = 2/7 k_n$.

Adhesion Force

When two materials are brought into each others vicinity, they exert an attracting force onto each other. This force is referred to as the adhesion force. Hamaker's theory for the attractive force between two spherical bodies with radii R_1 and R_2 as a function of the distance d, leads to the equation

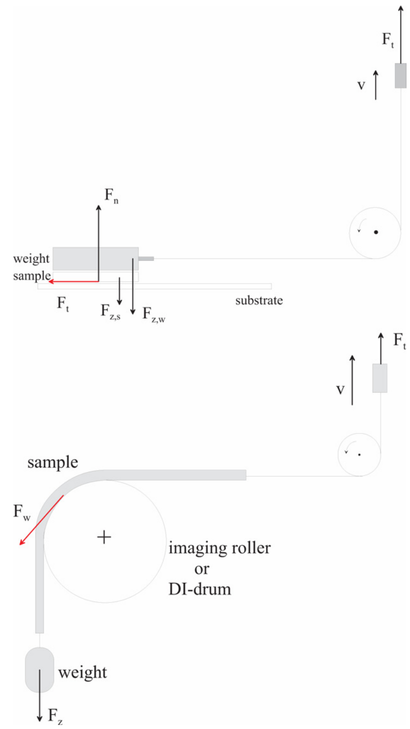

Figure 5. A schematic drawing of the experimental setups for the determination of the friction coefficient.

$$F_{adh} = \frac{A R_1 R_2}{12 (R_1 + R_2) d^2},$$

where A is known as the Hamaker coefficient. A solid boundary is modeled as a particle by letting R_2 go to infinity. The Hamaker coefficient is a material property. For toner, it is determined by atomic force microscopy and the centrifugal detachment method.

Magnetic Force

The general expression for the magnetic force $\mathbf{F}_{mag}$ is

$$\mathbf{F}_{mag} = (\mathbf{m} \cdot \nabla)\mathbf{B},$$

with $\mathbf{m}$ the magnetic moment of the particle and $\mathbf{B}$ the external magnetic induction. The magnetic moment $\mathbf{m}$ of a toner particle i depends on the external magnetic field. In the DI toner assembly the magnetic field originates from two sources: the field from the magnets within the imaging roller $\mathbf{B}_m$ and the field from the magnetized, surrounding toner particles $\mathbf{B}_a$. So, in general, we can write

$$\mathbf{F}_{mag} = (\mathbf{m} \cdot \nabla)\mathbf{B}\ (\mathbf{B}_m + \mathbf{B}_a).$$

The magnetic field $\mathbf{B}_m$ of the magnet within the imaging roller is calculated with Flux2D.[2] The interparticle magnetic force originating from $\mathbf{B}_a$, also called dipole-dipole force, is calculated as if a single magnetizable particle were present in each toner particle with the same magnetic dipole moment $\mathbf{m}$ as the whole toner particle. The magnetic properties of color and black toner are determined with a vibrating sample magnetometer (VSM).

Electric Force

To enable electric field toner development, the electric force exerted on the toner particle by the externally applied field strength on the toner particle must be larger than the magnetic force on that particle. Unfortunately, because of their quadratic nature, electric forces cannot be determined by superposition. We adopt here the approach of [8, 1] and use bi-spherical coordinates to solve the problem of a conducting toner particle in the field of an electrode. We consider a grounded sphere of radius R at a distance d from a plate on a voltage V; see Figure 6. This electrostatic problem can best be described in bi-spherical coordinates ξ, η, ϕ. The problem for the potential $u^*(\xi,\eta) = u(\xi,\eta) - V$ is given by ($\eta = \eta_0$ is the surface of the sphere)

$$\begin{aligned} &\nabla^2 u^* = 0, && (\xi,\eta) \in G, \\ &u^* = 0, && 0 < \xi < \pi, \eta = 0, \\ &u^* = -V, && 0 < \xi < \pi, \eta = \eta_0, \\ &\frac{\partial u^*}{\partial \xi} = 0, && \{\xi = 0 \vee \xi = \pi\}, 0 < \eta < \eta_0, \end{aligned}$$

in the problem region G, with

$$G = \{(\xi,\eta) 0 < \xi < \pi,\ 0 < \eta < \eta_0\}.$$

The solution is given by

$$u^* = -V\sqrt{2}\left(\cosh\eta - \cos\xi\right)^{\frac{1}{2}} \cdot \sum_{n=0}^{\infty} e^{-\left(n+\frac{1}{2}\right)\eta_0} \frac{\sinh\left(n+\frac{1}{2}\right)\eta}{\sinh\left(n+\frac{1}{2}\right)\eta_0} P_n(\cos\xi).$$

The electrostatic force F on the sphere is directed towards the plane $x = 0$, and given by (here S is the surface $\eta = \eta_0$ of the sphere)

$$F = -\int_S \sigma E_x dS.$$

We can write this integral as two separate integrals

$$F = \frac{4\pi\varepsilon_0 V^2}{\left(\sinh\eta_0\right)^2}\left(F_1 + F_2\right),$$

with

$$F_1 = \sum_{n=0}^{\infty} \frac{\cosh\left(n+\frac{1}{2}\right)\eta_0}{\sinh\left(n+\frac{1}{2}\right)\eta_0} e^{-(2n+1)\eta_0} \cdot \sinh\eta_0\left(ne^{\eta_0} - (n+1)e^{-\eta_0}\right),$$

and

$$F_2 = \sum_{n=0}^{\infty} \frac{\cosh\left(n+\frac{1}{2}\right)\eta_0}{\sinh\left(n+\frac{1}{2}\right)\eta_0} e^{-\left(n+\frac{1}{2}\right)\eta_0} \cdot \left[-\left(n+\frac{1}{2}\right)\frac{\cosh\left(n+\frac{1}{2}\right)\eta_0}{\sinh\left(n+\frac{1}{2}\right)\eta_0} e^{-\left(n+\frac{1}{2}\right)\eta_0} + (n+1)\cosh\eta_0 \frac{\cosh(n+3/2)\eta_0}{\sinh(n+3/2)\eta_0} e^{-(n+3/2)\eta_0}\right].$$

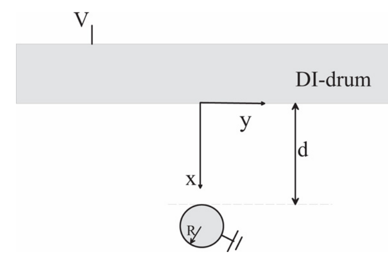

Figure 6. A grounded sphere at a distance d from a plate on voltage V.

Charge Model

When a pixel has to be printed, a voltage difference is applied between the imaging roller and a track in the DI-drum. This voltage difference causes toner particles in the DI toner assembly to get charged and to experience an electric force towards the DI-drum that is bigger than the magnetic force towards the imaging roller. A SiO_x layer, a dielectric layer above the conducting tracks, makes sure that the electric charge on the toner does not leak to the conducting tracks. Due to the dynamics of the DI toner assembly conducting paths are formed and broken. The conducting paths consist of toner-toner contacts and toner-imaging roller contacts. We treat the contact between a toner particle and another toner particle as an ideal electric resistance R_{tt}. Similarly the contact between a toner particle and the imaging roller is treated as an ideal electric resistance R_{ti}. A toner particle that comes in the vicinity of the DI-drum builds up charge and therefore an electric force towards the DI-drum. Toner particles within a certain range of the DI-drum are treated as a capacitor with respect to the DI-drum. The capacity is denoted by C_{td}. Particles that are in contact with the DI-drum also build up charge, but have some charge leakage through the SiO_x layer into the DI-drum too. The contact of a toner particle with the DI-drum is treated as a capacitor C_{td} in parallel with an ideal resistance R_{td}. By this routine a simulation geometry can be transferred into an electric circuit. An example of such a replacement electric circuit can be found in Figure 7. There are several methods[6] available to analyze a resistive network such as Figure 7. Our approach consists of a 1dimensional analysis of the electric circuit. We assume that the charging of toner particles is mainly due to a flow of charge through the shortest conductive path formed to the imaging roller. This shortest path is calculated for every particle and is translated to a 1-dimensional electric circuit. The equations of the 1-dimensional electric circuit can easily be solved.

Results

In general we are now able to calculate and visualize the behavior of the DI toner assembly, which consists of at most 10,000 particles, for a time frame of about 15ms in approximately one night on a PC. As an example we will show here the results for printed dots. Printed dots, also referred to as pixels, do not have perfectly sharp edges, see Figure 8. The quality of pixels can be expressed in terms of edge sharpness. Edge sharpness is determined from the coverage profile on the DI-drum. The coverage profile expresses the toner coverage of a pixel or line as a function of one of the directions. Distinction can be made between normal edge sharpness r_n in the direction of the ring electrodes of the DI-drum and axial edge sharpness r_a directed perpendicular to the ring electrodes of the DI-drum. Edge sharpness is defined as the distance in micrometers over which the coverage in an edge changes from 10% to 90%, where the maximum coverage in a pixel is scaled to 100%. As mentioned, we aim at a simulation tool that has quantitative agreement with experimental results. The ultimate goal is a tool that can predict aspects of print quality correctly. The normal edge sharpness r_n can be split in sharpness of the front edge $r_{n,f}$ and sharpness of the back edge $r_{n,a}$. We will show as an example case the results for the normal edge sharpness when applying DEM for the settings of the black development unit of the Océ CPS700. A total number of fifty simulations were run, where in each simulation a line was printed. From these fifty printed lines an average coverage curve is calculated. From this average curve a sigmoid fit is calculated. The sigmoid fit and the experimetally determined coverage profile for the black unit of the Océ CPS700 are displayed in Figure 9. It can be seen that there is good agreement between the experimental results and the simulation results.

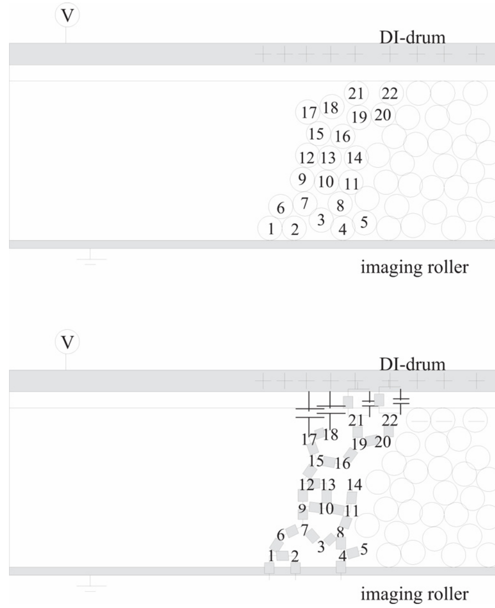

Figure 7. The electric circuit that models the charging behavior of the depicted geometry of the DI toner assembly.

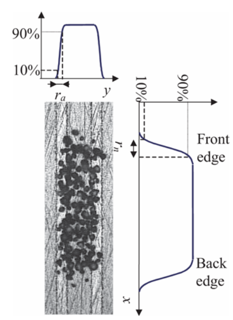

Figure 8. CCD recording of a pixel on the surface of a DI-drum with average coverage profiles (averaged over large number of pixels).

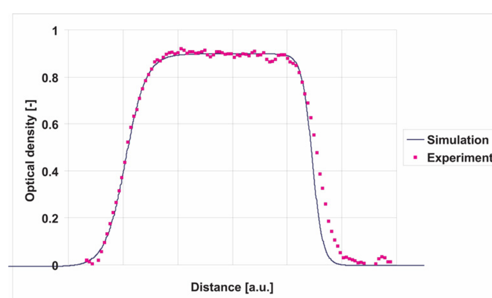

Figure 9. The calculated and measured average coverage curve for the black unit of the Océ CPS700.

Conclusion

The discrete element method has been used for simulating the behavior of the DI toner assembly in the development nip of the Océ Direct Imaging print process. It is shown that by determining the appropriate interaction rules and the associated parameters, it is possible to gain quantitative agreement between experimental and simulation results, even on important aspects as print quality.

References

1. Berry, J. S., Electrostatic forces on a conducting sphere due to a charge on a dielectric half-space, J. Phys. A: Math. Gen 9, 1939-1945 (1976).
2. Cedrat, Flux2D, http://www.cedrat.com.
3. Cundall, P. A., A computer model for simulating progressive large scale movements in block rock systems, Proc. Symp. Int. Soc. Rock Mech. 2, (1971).
4. Cundall, P.A. and Strack, O.D.L, Géotechnique 29, 47 (1979).
5. Hertz, H., Uber die Berührung fester elastischer Körper, Journal für die Reine und Angewandte Mathematik 92, 156-171 (1882).
6. Rizzoni, G., Principles and Applications of Electrical Engineering, McGraw-Hill, New York (2003).
7. Schafer, J., Rohrfluss granularer Materie: Theorie und Simulationen, PhD thesis, Gerhard Mercator Universit¨at, Duisburg (1996).
8. Warren, W.E. and Cuthrell, R.E., Electrostatic forces between conducting spheres at constant potential, Journal of Applied Physics 46, 45974599 (1975).

Biography

Ivo Severens received his M.Sc. degree in Mathematics from the Eindhoven University of Technology, the Netherlands, in 2001. Since then he has worked at Océ's Research and Development laboratory in Venlo in the field of toner development.